

Fabrication and Performance of Inverted Organic Solar Cells

Tyler J. Perlenfein
Department of Chemical and Biological Engineering,
Drexel University,
Philadelphia, PA

Dr. Jason B. Baxter
Department of Chemical and Biological Engineering,
Drexel University,
Philadelphia, PA

Fabrication and Performance of Inverted Organic Solar Cells

Abstract:

The present challenge of the photovoltaics industry is overcoming the large expenses associated with materials and processing. High vacuum and high temperature processing is a major factor affecting the cost of traditional solar cells. Solution-based processing of cheaper semiconductor materials (using spin coating, inkjet printing, screen printing, etc.) at low temperatures is an attractive method of cost reduction. Therefore the photovoltaic properties of the semiconducting polymer poly(3-hexylthiophene) (P3HT) blended with phenyl-C61-butryic acid methyl ester (PCBM) was investigated. Starting with conductive ITO-coated glass substrate, a thin layer of titanium oxide (TiO_x) was spin coated and annealed. A blend of P3HT and PCBM was then spin coated onto the TiO_x, forming the active layer. Gold contacts were evaporated to complete the inverted cell structure, which is more stable in air than conventional solar cells. The cells were characterized by taking current versus voltage and current versus wavelength curves, along with light harvesting efficiency data. Baseline quantum efficiencies, fill factors, and power conversion efficiencies were established for these cells. Active layer thickness, annealing times, and annealing temperatures were varied in order to optimize both light harvesting efficiency, short circuit current, and fill factor. A thin electron blocking layer of poly(ethylenedioxythiophene) doped with poly(styrene sulfonic acid) (PEDOT:PSS) was deposited on top of the active layer before electrode evaporation to improve the short circuit current by increasing the selectivity of the contact to holes while blocking electrons. Cell efficiency increased over the first 30 minutes of light exposure and also over several days of exposure to air. The short circuit current of this cell peaked at 8.2 mA/cm². With an open circuit voltage of 535 mV and fill factor of 43.5%, this cell had an efficiency of 1.91%. A light harvesting efficiency peak of 88.8% was obtained for the best-performing cell, but internal quantum efficiencies only 50%, indicating that efficiency is limited either by exciton dissociation or charge collection. Using layers of PEDOT:PSS increased the fill factor and photovoltage, however the desired effect of this layer on short circuit current has not yet been observed. Further work in the area of polymer photovoltaics will hopefully see high enough efficiencies to warrant industrial-scale applications.

Introduction:

The field of organic photovoltaics (OPVs) is growing very quickly in the scientific community. Between the years of 2002 and 2010, there were 1032 papers published in scientific journals worldwide concerning OPV cells with the P3HT:PCBM bulk heterojunction structure, with growing numbers from years to year.^[1] This is mostly due to the high potential of these products for large-scale industrial applications. Solution-based processing at low temperature is a key attribute of this field, making it compatible with large-throughput, high yield processes. While OPVs currently show power conversion efficiencies in the 3-6% range, this field of photovoltaics is still young and there are many aspects of OPVs that are not well understood or not fully explored. Studies that focus on reducing bulk and interfacial charge recombination, improving the carrier lifetimes in the bulk, and improving the charge collection characteristics of the cell through nanostructuring various layers all have potential to increase the average efficiency of OPV cells.

The operation of the OPV cell begins in the photoactive layer, which is comprised of semiconducting extended polymer chains blended with fullerenes. An incident photon of correct energy creates an exciton upon absorption, which diffuses through the active layer until either the electron or hole is conducted away or the two recombine. Charge separation happens when the electron-hole pair reaches an interface with a material of differing band energies. Because of the relatively short exciton diffusion lengths in most polymers (~10 nm), it is helpful to lessen the distance that the exciton must travel to reach this interface. Thus, the bulk heterojunction OPV was introduced in which donors and acceptors are intimately blended, creating interpenetrating nanoscale domains of electron and hole conducting materials. The most popular blend to date is P3HT (hole-conducting) and PCBM (electron-conducting).

The OPV cell is traditionally manufactured in the following manner: a layer of PEDOT:PSS is deposited on top of transparent, conducting indium tin oxide (ITO) by many different kinds of solution-based processing techniques. This forms an electron-blocking layer that helps to prevent leakage currents from developing in the counter electron flow direction. The active layer composed of P3HT:PCBM is then deposited on top of the PEDOT:PSS, again through some kind of solution process. Normally, a transparent, thin layer (~1 nm) of lithium fluoride is then deposited on top of the active layer which promotes electron flow and blocks hole transport. Finally, a low work function metal is deposited on top of the TCO to complete the cell. Problems with stability arise in this cell configuration, however. The acidity of the PEDOT:PSS layer tends to corrode the ITO or FTO, reducing charge collection capabilities. Any moisture which permeates the PEDOT:PSS layer tends to form insulating oxides which can greatly increase the series resistance of the cell. Finally, the low work function top electrode (traditionally aluminum) is readily oxidized which also increases the resistance of the cell.

In response to the stability challenges of the traditional OPV cell architecture, researchers have developed a so-called "inverted structure" in which the layer deposition order is reversed, with the lowest work function layers being deposited on top of the ITO substrate first. In this cell scheme, the oxide hole-blocking layer is deposited on the ITO, followed by the active layer. The electron blocking layer (either PEDOT:PSS or a group VB or VIB transition metal oxide) is then deposited. Following this is the deposition of a high work function metal (gold or silver) to complete the cell. This type of cell structure offers much greater air stability than the traditional type, due to a few contributing factors. The PEDOT:PSS is not in direct contact with the ITO, thereby eliminating the corrosion in the ITO layer. Also, the aluminum contact is replaced by a higher work function metal, which takes much longer to form surface oxide layers.

This work focuses on fabrication and characterization of OPV cells using the inverted structure. ITO substrates were coated in either ZnO or TiO_x, followed by deposition of a P3HT:PCBM layer and gold or silver electrode. Cells were produced with and without the PEDOT:PSS layer between the active layer and metal electrode. An emphasis was made on low-temperature solution processing of each layer (with exception of the metal electrode) in order to be consistent with the requirements of large scale industry.

Cells were characterized by I-V performance, absorbance spectroscopy, chronoamperometry, and scanning electron microscopy. Studies were conducted in order to optimize performance of the OPV cell, including: looking at effects of different oxide layers, changing the thickness of the active layer, effects of the presence of a PEDOT:PSS layer, effect of annealing times, looking at air stability over a period of a few days, and effects of light exposure over a period of up to an hour.

Experimental:

ITO coated glass sheets (~120 nm thickness, Colorado Concept Coatings) were first cleaned via sonication in heated acetone, 3% soap solution, then isopropanol. The panels were removed and dried with nitrogen gas before coating. For ZnO layers, the precursor solution was composed of .375 M zinc acetate with equimolar ethanolamine in anhydrous ethanol solvent (Sigma Aldrich). The solution was heated to 60 °C and stirred for 4 hours until it became clear.

Zno layers were prepared via dip coating ITO panels in the precursor solution at a speed of 200 mm/min and relative humidity below 15%. The panels were subsequently transferred to a glove box through which nitrogen gas was flowing. The gas was held at 32% relative humidity. The panels were annealed at 400 °C for 20 min under these conditions.

TiO_x layers were prepared using a precursor solution composed of 1 wt% titanium isopropoxide (TTIP) in anhydrous 2-propanol (Sigma Aldrich).

TiO_x layers were spin coated using approximately 200 μL of the precursor solution on ITO panels at 2000 rpm for 30 seconds. The panels were allowed to sit in air for one hour, then annealed at 150 °C for ten minutes to fully hydrolyze the TTIP into TiO_x.^[2]

Active layer solution was composed of a 2.4 wt% blend of equal mass parts P3HT (Merck M101) and PCBM (American Dye Source) in chlorobenzene. This solution was heated to 100 °C for approximately 15 seconds to aid in solute dissolution, then removed from the heat and stirred overnight. Immediately prior to use, the solution was sonicated for 10 minutes in a room temperature bath, then loaded into a syringe and strained through a 0.45 μm PVDF syringe filter upon dispensing.

The active layer was deposited onto ZnO or TiO_x layers by spin coating the P3HT:PCBM solution at 500, 1000, 1500, 2000, and 2500 rpm for 50 seconds. ITO for back contacts was exposed by swabbing strips of the active area with chlorobenzene. The panels were then annealed at 170 °C for times of 1, 5, or 10 minutes.^[3]

PEDOT:PSS (Clevios P VP AI 4083) was prepared for deposition by mixing with methanol. In undiluted form, the water-based PEDOT:PSS does not wet the surface of the active layer. The addition of 2 volume parts methanol to 1 volume part PEDOT:PSS decreases the surface energy of the drop/active layer interface and allows for better wetting to take place.

PEDOT:PSS was deposited by spin coating at 2000 rpm for 4 minutes. After deposition, a thin strip of ITO was exposed by swabbing with hot water (approximately 80 °C). The panels were then annealed at 90 °C for 30 minutes in order to drive out the resident water in the PEDOT:PSS layer and to improve the contact between this layer and the active layer.^[4]

Immediately after the panels had cooled to room temperature, masks were applied and the panels were loaded into the thermal evaporator. Gold or silver electrodes were deposited at a rate of 1 Å/s in a vacuum of 5×10^{-5} torr.

After evaporating, data was taken on the cells over a period of a few days. Transient photocurrent behavior was studied by light illumination for up to 30 minutes.

Results:

It was found that cells using a ZnO layer as a TCO showed an initial photocurrent of 2.4 mA/cm², which rapidly degraded upon exposure to light by up to 50% over a 30 minutes exposure period. Cells that used TiOx instead of ZnO were found to have initial photocurrents of 0.1 mA/cm², which improved with light exposure over a period of 30 minutes to 4.2 mA/cm². This increase in photocurrent is attributed to free electrons in the TiOx layer filling trap states, allowing other electrons to pass through unhindered. Oxygen scavenged from air during the period of film development is also thought to increase the conductivity of this layer.^[5] Initial I-V curves for ZnO under light intensity of 100 mW/cm² showed Voc of 420 mV, a fill factor of 41.2%, and a power conversion efficiency of 0.5%. TiOx cells, under the same light intensity and after a 30 minute exposure period, showed a Voc of 500 mV, FF of 48.5%, and PCE of 1.03%.

When altering the spin coating speed during deposition of the active layer, it was found that a speed of 500 rpm produced the thickest layers and showed the highest amount of absorbance, which peaked at OD of 0.8. Though still lower speeds would produce thicker layers, a practical limit on the active layer thickness is imposed due to non-uniformities that arise at slower speeds.

The annealing time had a significant impact on the cell performance. The results of this test are shown in Table I.

Annealing Time (min)	Jsc (mA/cm2)	Voc (mV)	FF	Eff
1	5.46	470	36.46%	0.93%
5	4.26	500	48.50%	1.03%
10	3.64	530	41.12%	0.79%

Table I. Annealing time study of TiOx-based cells.

It can be seen that the most short circuit current is derived from cells with the smallest P3HT and PCBM domain sizes, as governed by anneal time. This is attributed to the higher internal quantum efficiencies caused by the larger interfacial area in the active layer. The performance of these cells are limited by an inflection point in the I-V curves and low shunt resistance. The highest cell efficiency is observed after annealing for 5 minutes. The fill factor of the cell is increased due to the disappearance of the inflection point after annealing. Longer annealing leads to slightly larger domains, which improves charge transport at the possible expense of charge separation.

PEDOT:PSS was shown to have a relatively small effect on the OPV cells. The results are shown in Table II.

	Jsc (mA/cm ²)	Voc (mV)	FF	PCE
no PEDOT:PSS	3.71	500	42.10%	0.78%
PEDOT:PSS	4.01	515	38.90%	0.80%

Table II. Effect of PEDOT:PSS Layer.

It can be seen from Table II that the inclusion of a PEDOT:PSS layer did relatively little to increase the attributes of the cell. This seems to contradict current literature and could be due to poor adhesion of the PEDOT:PSS layer on the active layer, causing little or no deposition.

It was shown that the performance of the TiO_x-based cells improved over both light exposure and a period of aging in air for a few days.

Exposure Time (min)	Jsc (mA/cm ²)	Voc (mV)	FF	PCE
1	0.61	185	30.50%	0.04%
5	3.26	370	31.20%	0.37%
20	3.4	410	31.60%	0.45%
30	3.4	470	34.60%	0.55%

Table III. Light exposure study with TiO_x on day 1.

Table III shows the effect of exposing the TiO_x cells to light. In each study, the light intensity was the same as the testing conditions of 100 mW/cm². As can be seen, the short circuit current reaches a steady-state value at approximately 30 minutes of exposure, and cell performance approaches a maximum value. The data in Table III is taken on the day of cell fabrication. These same cells were tested again after aging for 2 days in air. After another 30 minutes of light exposure, the I-V sweep showed Jsc values around 4.1 mA/cm², Voc of 510 mV, FF of 38.9%, and PCE of 0.8%. This trend of improved cell performance after aging has been demonstrated with multiple batches of OPV cells.

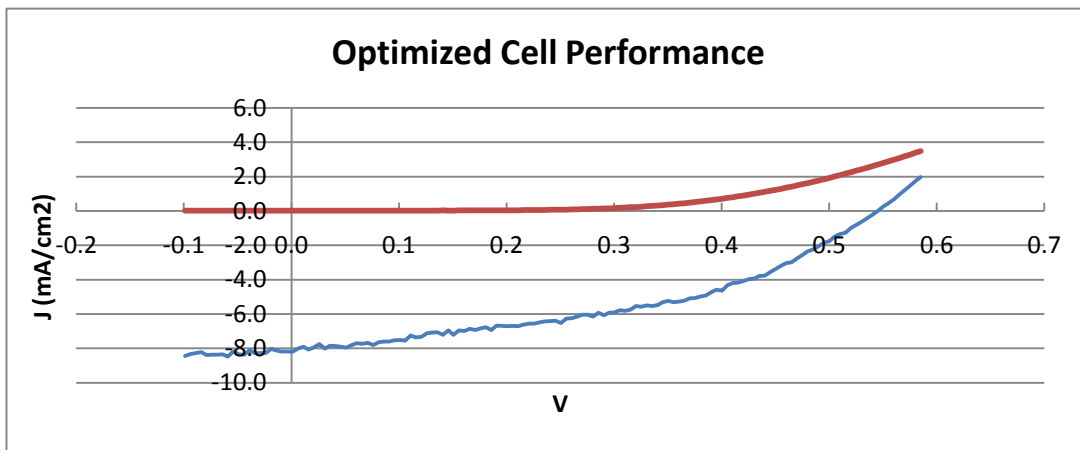


Figure I. Light and dark curves showing optimized cell performance.

The best-performing cells produced after optimization showed a Jsc of 8.2 mA/cm², Voc of 535 mV, FF of 43.5%, and PCE of 1.91%.

Though OPV solar cells are markedly less efficient than others in the industry, notably mono- and polycrystalline silicon, this type of cell shows great promise in its potential to significantly lower the manufacturing and materials cost of the solar industry, and to provide a more flexible product to consumers.

Acknowledgements:

Funding for this project was provided by the Energy Commercialization Institute, Ben Franklin Technology Partners of Southeastern Pennsylvania.

This work would not have been possible without the guidance and support of principle investigator Dr. Jason Baxter. The author would also like to thank Hasti Majidi, Borirak Opananont, Glenn Guglietta, and Siamak Nejati for their generous and helpful advice.

References:

- [1] M. Dang, L. Hirsch, G. Wantz, *Adv. Mater.* 2011, 23, 3597–3602.
- [2] J. Kim, K. Allen, S. Oh, S. Lee, M. Toney, Y. Kim, C. Kagan, C. Nuckolls, Y. Loo, *Chem. Mater.*, Vol. 22, No. 20, 2010.
- [3] C. Kim, S. Lee, E. Gomez, J. Kim, Y. Loo, *Appl. Phys. Lett.* 94, 113302, 2009.
- [4] Krebs, *Polymer Photovoltaics: A Practical Approach*. SPIE Press, 2008.
- [5] K. Lee, J. Kim, S. Park, S. Kim, S. Cho, A. Heeger, *Adv. Mater.* 2007, 19, 2445–2449.F.